



## Original article

# Experimental study on the tension-tension fatigue behaviour of glass/epoxy quasi-isotropic composites

N.H. Padmaraj<sup>a</sup>, Kini M. Vijaya<sup>b</sup>, Pai Dayananda<sup>a,\*</sup>

<sup>a</sup> Department of Aeronautical and Automobile Engineering, Manipal Institute of Technology, Manipal Academy of Higher Education, Manipal 576104, India

<sup>b</sup> Department of Mechanical and Manufacturing Engineering, Manipal Institute of Technology, Manipal Academy of Higher Education, Manipal 576104, India



## ARTICLE INFO

## Article history:

Received 13 November 2018

Accepted 28 April 2019

Available online 30 April 2019

## Keywords:

Fatigue damage

Quasi-isotropic

Stiffness

Stress ratio

Frequency

## ABSTRACT

This study investigates the tension-tension fatigue behaviour of glass/epoxy quasi-isotropic laminates. Constant amplitude tension-tension fatigue tests were performed at different stress level at a stress ratio,  $R = 0.1$  and at a frequency of 3 Hz. The damage growth in the material was characterized by evaluating the degradation in stiffness. A phenomenological cumulative stiffness degradation based damage model was used to predict the damage development in the material. It was observed that, in the initial fatigue loading cycle, the material exhibited rapid reduction in stiffness and maintained a constant rate of degradation until failure.

© 2019 The Authors. Production and hosting by Elsevier B.V. on behalf of King Saud University. This is an open access article under the CC BY-NC-ND license (<http://creativecommons.org/licenses/by-nc-nd/4.0/>).

## 1. Introduction

Fibre reinforced polymers (FRP) are being used extensively in structural applications subjected to fatigue loading. In fatigue loading, materials are subjected to cyclic stresses below their ultimate tensile strength. Application of repeated cyclic stresses will develop micro cracks in the material resulting in degradation of the mechanical properties. Fatigue failure phenomenon in homogenous materials initiates from single micro crack and propagates perpendicular to the direction of loading (Ramesh Talreja, 2016; Reifsnider, 1991). The crack initiation and propagation in homogenous materials is quantified by strain-life approach. Fatigue failure is characterised by multiple damage modes such as matrix cracking, Fibre/matrix interface debonding and fibre failure (Hahn, 1979; Ansari et al., 2018). Damage developed during the fatigue test is loading cycle dependent and during each cycle, damage accumulates in the form of micro cracks in different planes. Increasing the loading cycles, intensifies the damage and results in degradation of strength and stiffness of the material. The extent

of damage severity in multidirectional laminates is quantified by understanding the rate of degradation in stiffness of the material (Ramesh Talreja, 2016; Zong and Yao, 2017; Liu et al., 2018; O'Brien et al., 1989). Reifsnider (1991) developed a multistage model to characterise the development of fatigue damage. As per the model, during the initial fatigue-loading period, damage is characterised by primary matrix cracking along the plies and reaches a saturation point. In the intermediate stage, crack grows in inter-laminar plies and leads to delamination of fibre matrix interface. In the final stage, cumulative damage grows rapidly, resulting in failure of the material. The damage development is also affected significantly by the loading frequency. In fatigue loading, higher testing frequency leads to increase in the laminate temperature. Rise of temperature increases the rate of degradation of stiffness and the damage growth. Fibre orientation and loading direction for composites showed significant effect on fatigue life. El Kadi and Ellyin (1994) studied the tension-tension (T-T) fatigue behaviour of glass/epoxy composite laminates and showed reduction of fatigue life with the increase of fibre orientation angle. The increment in the fibre orientation angle reduces the stiffness of the material and results in lower fatigue life. Fibre volume content and percentage of void content are the other two factors that directly influence the fatigue damage growth rate of the material (Maragoni et al., 2017). Analysis of effect of fibre content on T-T fatigue behaviour of carbon/epoxy laminates showed that an increase in fibre volume fraction from 30 to 55% resulted in an increment in the fatigue life by 40% (Brunbauer et al., 2015). Reviewed literature indicates that developing mathematical mod-

\* Corresponding author.

E-mail address: [dayanand.pai@manipal.edu](mailto:dayanand.pai@manipal.edu) (P. Dayananda).

Peer review under responsibility of King Saud University.



Production and hosting by Elsevier

els to predict the fatigue damage growth rate is a complex phenomenon. Mao and Mahadevan (2002) proposed nonlinear damage model based on experimental results. The study showed that applied number of cycles and degradation of stiffness can be used to predict the cumulative damage of the material. Toubal et al., (2006) developed a cumulative damage model for carbon/epoxy laminates by correlating stiffness and number of cycles.

Present work investigates the fatigue behaviour of quasi-isotropic glass/epoxy composite laminates fabricated with a stacking sequence of  $[0/90/+45/-45]_s$ . An experimental analysis was carried out at different stress levels using axial T-T fatigue loading mode at a stress ratio,  $R = 0.1$  and at a frequency of 3 Hz. Fatigue life of the material is presented using S-N plot and damage accumulated in the laminates is predicted by monitoring stiffness loss of the material. Existing non-linear damage prediction mathematical model was adopted to understand the propagation of fatigue damage. Scanning electron microscopic images were used to understand the fracture behaviour of the composites.

## 2. Experiment details

### 2.1. Materials and methods

The quasi-isotropic composite laminates were fabricated by vacuum bagging technique. The specimen were reinforced with unidirectional (UD) E-glass fabric (310 GSM) having a density of  $2.54 \text{ g/cm}^3$  and were procured from CFW New Delhi, India. Lapox L12 (Atul grade) with a density of  $1.12 \text{ g/cm}^3$  and K-6 hardener (amine group) used as thermoset matrix material. The laminates with a Fibre weight fraction of 55% having eight layers of UD E-glass fabric was prepared with a stacking sequence of  $[0/90/+45/-45]_s$ . The experimental density of the specimen was measured using Archimedes principle and found to be  $1.54 \text{ g/cm}^3$  as reported in (Pavan Acharya et al., 2018). The specimens for static tensile test and for T-T fatigue test were prepared as per ASTM D 3039 with a gauge length of 190 mm and a gripping length of 30 mm on both sides and with a thickness of 3 mm (ASTM, 2014).

### 2.2. Tensile and fatigue test

Uni-axial static tensile tests were conducted using BiSS make Universal testing machine equipped with fatigue setup. To ensure repeatability; five samples with identical dimensions were used for tensile test. The tension-tension fatigue behaviour of the quasi-isotropic laminates were analysed in accordance with ASTM D 3479 (Demers, 1998). Tests were conducted in constant amplitude load mode and loading pattern controlled using sinusoidal waveform at a stress ratio,  $R = 0.1$ . The fatigue life of material is influenced by testing frequency; higher testing frequency results in self-heating of laminates (Ansari et al., 2018). To reduce the effect of self-heating tests were conducted at a frequency of 3 Hz. At 0.4 stress range, fatigue test were stopped at  $1 \times 10^6$  cycles and considered as run out specimens.

## 3. Results and discussion

### 3.1. Tension test

Tensile tests of quasi-isotropic laminates were conducted at ambient conditions and at a displacement rate of 2 mm/min. The stress-strain curve for specimens are shown in Fig. 1. The stress-strain curve obtained from the test clearly indicates the influence of fibre stacking sequence on failure characteristics of the laminate. The curve shows nonlinear elastic feature until the failure point and is considered as a bilinear curve. The intersection of two curves

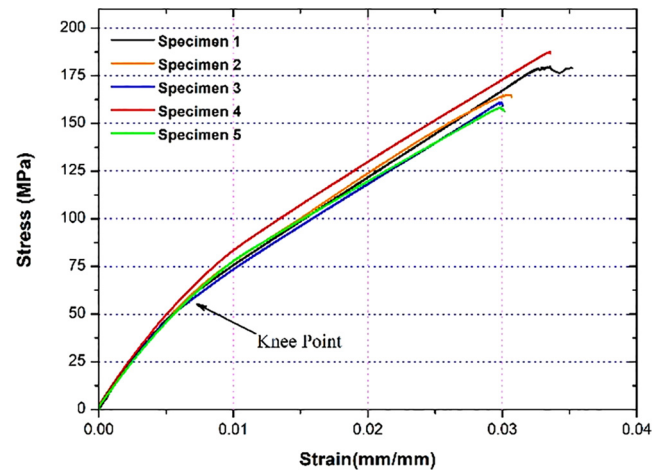


Fig. 1. Stress-Strain curve of quasi-isotropic laminate.

in Fig. 1 is known as knee point and represents the failure point of the plies perpendicular to the direction of loading (Sun and Zhou, 1988; Agarwal and Dally, 1975). The ultimate failure of the laminate occurs at fracture strain of fibre along the loading direction. Using the stress- strain curve average ultimate strength of the laminate was found to be 170.38 MPa and average failure strain was 3.2%. The bilinear pattern of stress-strain curve resulted in two tensile modulus  $E_1$  and  $E_2$ . Modulus,  $E_1$  of the curve obtained from the initial slope of the curve and found to be 7.96 GPa. Final modulus,  $E_2$  obtained above the knee point of the curve and estimated as 4.33 GPa which agrees with the published literatures (Reifsnider, 1991; Agarwal and Dally, 1975).

### 3.2. Fatigue test

The experimental results obtained from constant amplitude tension-tension fatigue test at different stress levels is shown in Table 1.

The number of cycles to failure obtained at 0.8-stress level shows large scattered data with a coefficient of variation of

Table 1  
Experimental values of tension-tension fatigue test of quasi-isotropic laminates.

Stress Level	Failure Cycles, N	Average failure cycle	Coefficient of variation in %
0.8	3170	2063	42.64
	1570		
	976		
	2710		
	1893		
0.7	9630	9806	29.27
	6141		
	8768		
	14,052		
	10,441		
0.6	547,672	84,090	20.48
	368,317		
	326,543		
	387,891		
	421,879		
0.5	767,845	620,427	25.94
	837,643		
	609,428		
	423,269		
	611,371		
0.4	1,001,231	Runout	Runout
	1,000,551		

42.64%. Number of cycles to failure obtained at lower stress levels shown low scattering as compared to 0.8-stress level. Fatigue data obtained from the experiments were analysed by the classical stress-life approach as per ASTM E739 (ASTM, 2012) and established S-N curve for laminates as shown in Fig. 2.

The testing process was terminated at  $1 \times 10^6$  cycles at 0.4 stress level as the laminates did not fail at this stress level. In S-N curve, these runouts are shown with an arrow. Experimental results of fatigue test were showed a linear fit based on the semi log linear relationship between stress level and the fatigue life as per Eq. (1) using linear regression analysis (Vieira et al., 2018; Zhao et al., 2016; Ertas and Sonmez, 2014).

$$\frac{\sigma_{\max}}{\sigma_u} = m \log N + b \tag{1}$$

where  $m = -0.110$  is the slope of the S-N curve and predicts the rate of degradation of the fatigue life of quasi-isotropic laminate. Parameter  $b > 1$ , is the one cycle intercept of the curve fitting and found to be 1.153. The obtained values agrees closely to the published results. The accuracy of the prediction represented by  $R^2 = 0.87304$  and found to be within the acceptable limit (Vieira et al., 2018; Li et al., 2015).

### 3.3. Fatigue damage accumulation

The fatigue damage developed in the composite materials is evaluated in terms of degradation in stiffness during fatigue loading. Stiffness of the material was estimated in equal intervals during fatigue loading to understand the damage growth behaviour. Fig. 3 shows the normalised stiffness degradation of the quasi-isotropic laminates at a stress level of 0.5, 0.6 and 0.7. Stiffness of the material experimentally evaluated in frequent intervals of fatigue loading from the stress-strain data for the corresponding loading cycle. Stiffness degradation behaviour can be described in three stages. In stage one, during the initial few loading cycles, rapid reduction in stiffness is observed. In second stage, stiffness reduces at a constant rate. Rapid reduction is observed near the failure in stage three. The specimen, which was loaded at stress level of 0.5, showed 50% reduction in stiffness at failure point. In the current study, quantitative evaluation of fatigue damage was carried out by monitoring reduction of stiffness in each cycle of the loading.

The damage developed in the material for each cycle during fatigue loading was evaluated using Eq. (2) (Mao and

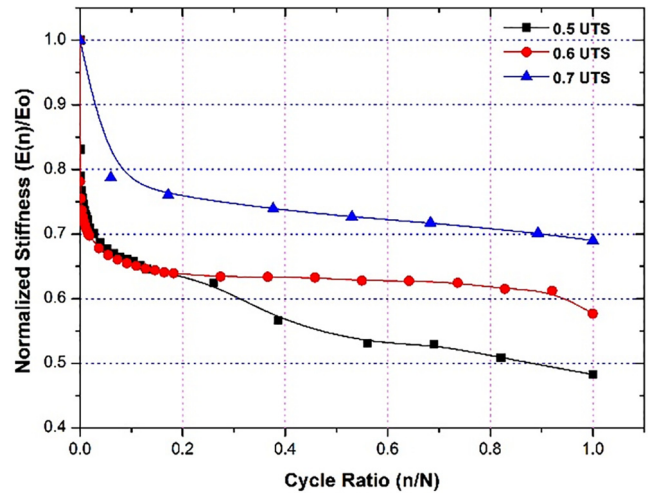


Fig. 3. Stiffness degradation at different stress level.

Mahadevan, 2002; Toubal et al., 2006; Venkatachalam and Murthy, 2018).

$$D = 1 - \frac{E_n}{E_o} \tag{2}$$

where  $D$  is the fatigue damage accumulated,  $E_o$  is the initial dynamic stiffness measured during the first loading cycle and  $E_n$  is the stiffness of the material after  $n$  number of cycles. Stiffness is the ratio of the corresponding stress and strain of the material during fatigue loading in each cycle. The experimental results shown in Fig. 3 indicated that the stiffness of the material at failure point is not zero and hence final fracture stiffness was incorporated (Venkatachalam and Murthy, 2018; Wu and Yao, 2010) in Eq. (2) as

$$D = \frac{E_o - E_n}{E_o - E_f} \tag{3}$$

Eq. (3) shows that the accumulated damage in the material varies from 0 to 1. The damage growth in specimen when they were subjected to fatigue loading at 0.7, 0.6 and 0.5 stress level is exhibited in Fig. 4. Damage estimated in each stress levels at frequent intervals of loading as per Eq. (3) by using experimental stress-strain data.

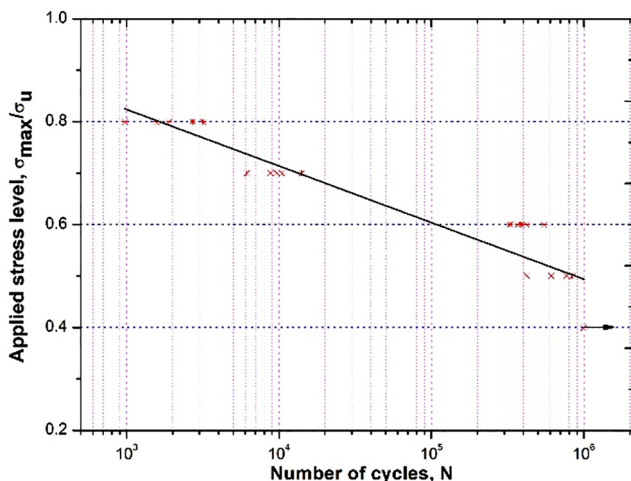


Fig. 2. S-N curve of quasi-isotropic laminate at a stress ratio of 0.1.

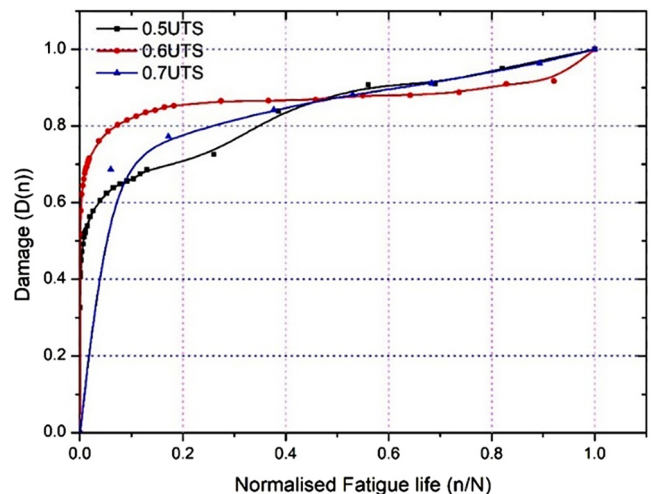


Fig. 4. Experimental damage evolution curve at different stress levels.

The damage growth mechanism in quasi-isotropic laminates is studied in three stages (Reifsnider, 1991). During initial stage micro cracks in the matrix parallel to the direction of fibre in multiple locations were developed. This damage grows rapidly and contributes to 60% of the total damage. The cracking process continues to achieve a saturation period and the cracking pattern in

the laminate is termed as characteristic damage state (CDS). In the intermediate stage; micro cracks developed during the initial stage merge and leads to debonding at fibre-matrix interface which results in inter-laminar cracks. Steady and slow damage growth rate is observed in second stage. The last stage shows rapid damage development process and which ultimately results in 0° oriented fibre failure of the laminates followed by longitudinal splitting and rupture of fibre surface (Reifsnider, 1991; Ansari et al., 2018; Zong and Yao, 2017; Mahato et al., 2018; Rafiee, 2017).

**Table 2**  
Material parameters of quasi-isotropic laminates for damage evolution at different stress levels.

Stress level, % of UTS	q	m <sub>1</sub>	m <sub>2</sub>	R <sup>2</sup>
0.7	0.9414	0.1124	4.688	1.0000
0.6	0.9259	0.06687	184.3	0.9889
0.5	0.8321	0.1045	1.039	0.9967

3.4. Analytical model for fatigue damage

The analytical damage growth model developed by Mao and Mahadevan (2002) is based on continuum damage mechanism. Eq. (4) is used to establish a relation between number of cycles

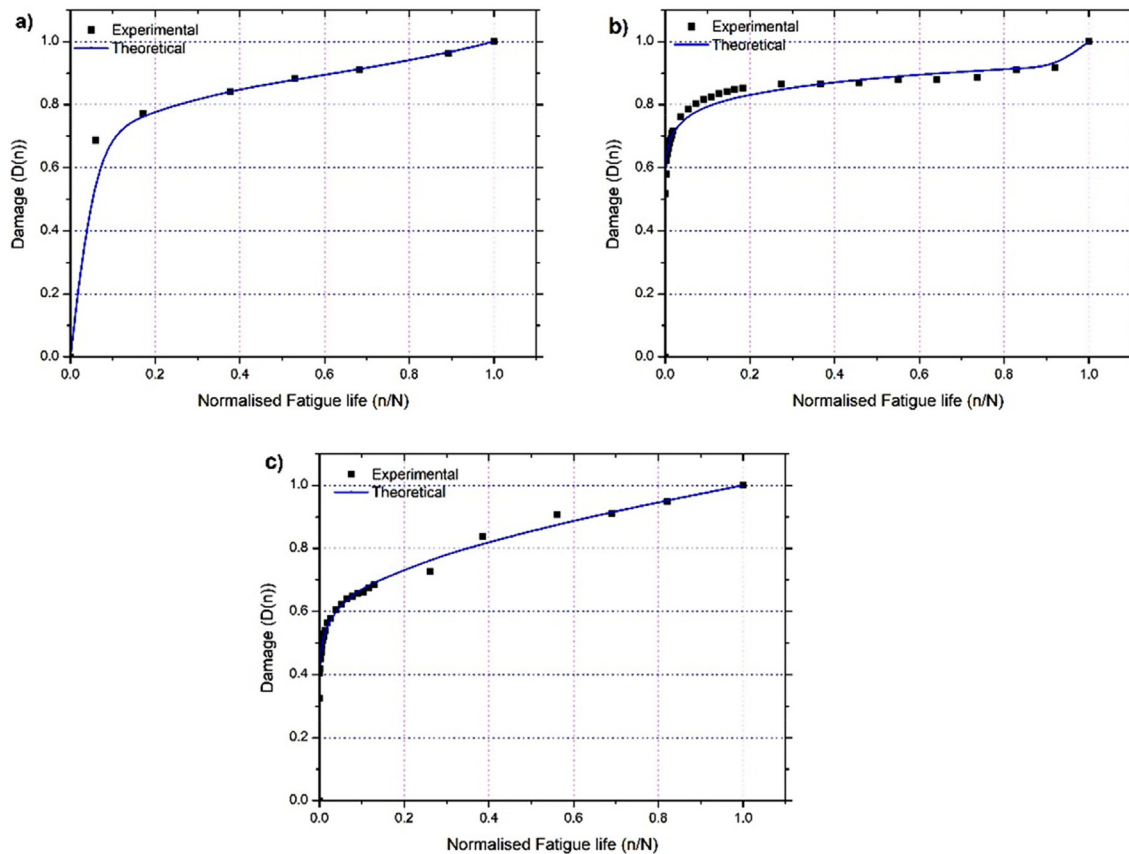


**Fig. 5.** Comparison of experimental and theoretical damage evolution at different stress level, (a) 0.7, (b) 0.6, (c) 0.5.

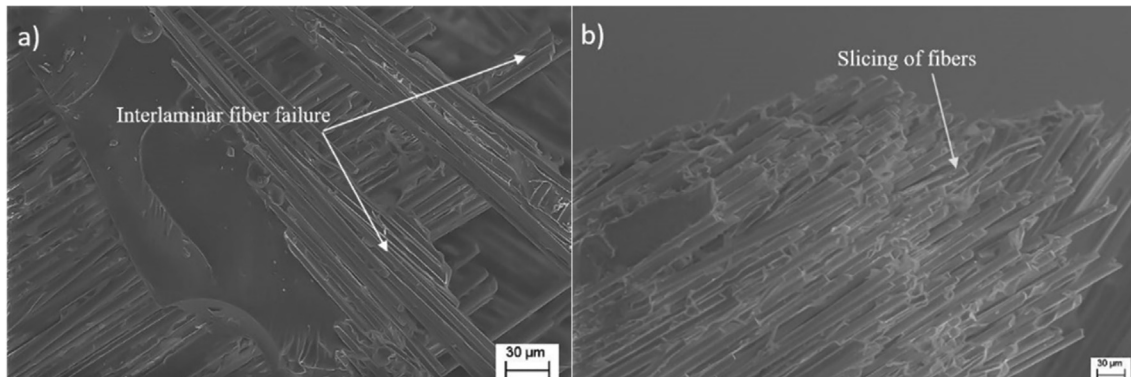


**Fig. 6.** SEM micrographs of static test fracture surface showing (a) Interlaminar Fibre failure, (b) Slicing of Fibre.

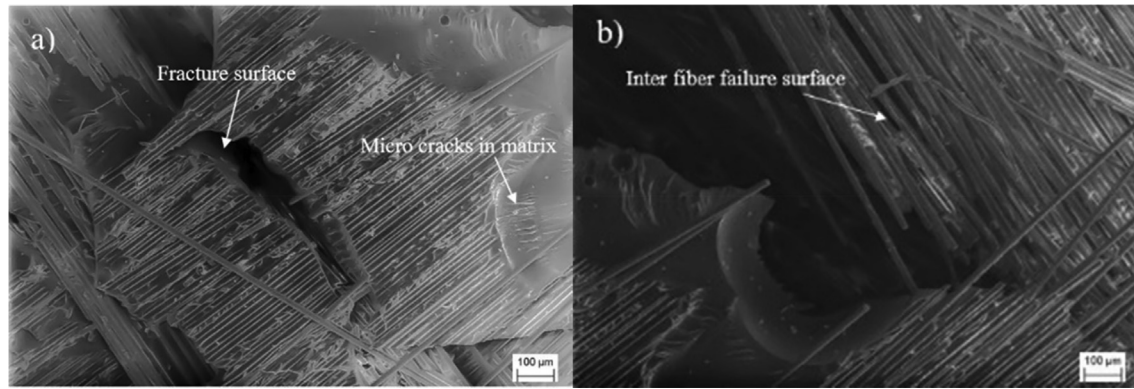


Fig. 7. SEM micrographs of fatigue fracture at 0.7 stress level showing (a) micro cracks in matrix, (b) delamination of Fibre matrix interface.

applied and damage developed at different stress levels (Toubal et al., 2006; Ziemian et al., 2016).

$$D = q \left( \frac{n}{N} \right)^{m_1} + (1 - q) \left( \frac{n}{N} \right)^{m_2} \quad (4)$$

where  $D$  is the accumulated damage,  $n$  is the applied number of cycle,  $N$  is the life of the material at corresponding cycles,  $m_1$ ,  $m_2$  and  $q$  are the material parameters. The first part of the Eq. (4) represents initial fatigue damage growth mechanism with  $m_1 < 1$  and second part of the equation represents the rapid damage growth phenomenon near the material failure cycles with  $m_2 > 1$ .  $q$  is the weighing parameter for different stress levels. Values of these parameters were extracted with the help of least square regression method in MAT LAB for different stress levels from the experimental fatigue data and damage data obtained using Eq. (3). Values of material parameters for different stress levels with coefficient of determination ( $R^2$ ) as a measure of quality of curve fitting is shown in Table 2. Fig. 5(a)–(c) shows the comparison of experimental and theoretical damage evolution characteristics of quasi-isotropic glass/epoxy composites,

### 3.5. SEM image analysis

The failure morphology of the specimen failed in static test was shown in Fig. 6(a) and (b) and specimen failure largely attributed to fibre failure. Brush like fracture surface with inter fibre bundle failure with delamination and large number of fibres pull out to the surface is observed. In addition, wedge shaped slicing of the fibre surface is observed. This indicates fibre dominant failure phenomenon.

Fig. 6(a) and (b) shows the fatigue fracture surface at 0.7 stress level. SEM images of fatigue fracture surface provided evidence of the delamination and the presence of micro cracks in the laminates. Smooth micro crack nucleation's is observed along matrix failure surface as shown in Fig. 7(a). In addition, multiple fragmentation between fibre and matrix interface is observed in fatigue loading as shown in Fig. 7(b). The fracture surface also shows matrix shear ridges and shows low fibre exposure; indicating matrix damage dominated failure. Presence of multiple micro cracks in the material resulted in catastrophic failure of the specimen.

## 4. Conclusions

Data on fatigue characterisation of quasi-isotropic glass/epoxy laminate under on axis tension-tension fatigue test at a stress ratio,  $R = 0.1$  and at a frequency of 3 Hz was presented in this paper. The static tensile properties of the composites largely depended on the

orientation of individual plies. The stress-strain curve showed non-linearity and hence represented as a bi-linear curve. Fibres normal to the loading direction failed at a lower fracture strain and complete failure of specimen occurred at the failure strain of fibres orientated along the loading direction. Damage growth in the laminates were characterized by understanding the degradation of stiffness of the material. In the initial fatigue, loading material showed rapid reduction in the stiffness and maintained a constant rate of degradation until the failure of the material. The existing cumulative damage model used to predict the damage growth rate in the material and the least square regression analysis carried out to obtain the material parameters at different stress levels. Scanning electron images were used to understand the difference between the static and fatigue failure of the specimens. The fractography images of specimen failed in fatigue test clearly showed presence of micro cracks and inter fibre surface delamination.

## Acknowledgements

The authors would like to acknowledge Advanced Composite Research Lab, Department of Aeronautical and Automobile Engineering, Manipal Institute of Technology, MAHE, Manipal, for the support provided for the fabrication and testing facility of composite materials.

## Conflict of interest

The authors declare that they have no conflict of interest.

## References

- Agarwal, B.D., Dally, J.W., 1975. Prediction of low-cycle fatigue behaviour of GFRP: an experimental approach. *J. Mater. Sci.* 10, 193–199. <https://doi.org/10.1007/BF00540342>.
- American Society For Testing and Materials, 2014. Standard test method for tensile properties of polymer matrix composite materials. *Annu. B. ASTM Stand.* 1–13. <https://doi.org/10.1520/D3039>.
- Ansari, M.T.A., Singh, K.K., Azam, M.S., 2018. Fatigue damage analysis of fiber-reinforced polymer composites—A review. *J. Reinf. Plast. Compos.* 37, 636–654. <https://doi.org/10.1177/0731684418754713>.
- ASTM, 2012. Standard Practice for Statistical Analysis of Linear or Linearized Stress-Life (S-N) and Strain-Life (ε-N) Fatigue Data 1. *Annu. B. ASTM Stand.* i 1–7. <https://doi.org/10.1520/E0739-10.2>.
- Brunbauer, J., Stadler, H., Pinter, G., 2015. Mechanical properties, fatigue damage and microstructure of carbon/epoxy laminates depending on fibre volume content. *Int. J. Fatigue* 70, 85–92. <https://doi.org/10.1016/j.ijfatigue.2014.08.007>.
- Demers, C.E., 1998. Tension-tension axial fatigue of E-glass fiber-reinforced polymeric composites: fatigue life diagram. *Constr. Build. Mater.* 12, 303–310. [https://doi.org/10.1016/S0950-0618\(98\)00007-5](https://doi.org/10.1016/S0950-0618(98)00007-5).
- El Kadi, H., Ellyin, F., 1994. Effect of stress ratio on the fatigue of unidirectional glass fibre/epoxy composite laminae. *Composites* 25, 917–924. [https://doi.org/10.1016/0010-4361\(94\)90107-4](https://doi.org/10.1016/0010-4361(94)90107-4).

- Ertas, A.H., Sonmez, F.O., 2014. Design optimization of fiber-reinforced laminates for maximum fatigue life. *J. Compos. Mater.* 48, 2493–2503. <https://doi.org/10.1177/0021998313499951>.
- Hahn, H.T., 1979. Fatigue behavior and life prediction of composite laminates. *Compos. Mater. Test. Des. Fifth Conf.*, 383–417.
- Li, D., Sen, Jiang, N., Zhao, C.Q., Jiang, L., Tan, Y., 2015. Experimental study on the tension fatigue behavior and failure mechanism of 3D multi-axial warp knitted composites. *Compos. Part B Eng.* 68, 126–135. <https://doi.org/10.1016/j.compositesb.2014.08.042>.
- Liu, H., Cui, H., Wen, W., Kang, H., 2018. Fatigue characterization of T300/924 polymer composites with voids under tension-tension and compression-compression cyclic loading. *Fatigue Fract. Eng. Mater. Struct.* 41, 597–610. <https://doi.org/10.1111/ffe.12721>.
- Mahato, K.K., Dutta, K., Ray, B.C., 2018. Static and dynamic behavior of fibrous polymeric composite materials at different environmental conditions. *J. Polym. Environ.* 26, 1024–1050. <https://doi.org/10.1007/s10924-017-1001-x>.
- Mao, H., Mahadevan, S., 2002. Fatigue damage modelling of composite materials. *Compos. Struct.* 58, 405–410. [https://doi.org/10.1016/S0263-8223\(02\)00126-5](https://doi.org/10.1016/S0263-8223(02)00126-5).
- Maragoni, L., Carraro, P.A., Peron, M., Quaresimin, M., 2017. Fatigue behaviour of glass/epoxy laminates in the presence of voids. *Int. J. Fatigue* 95, 18–28. <https://doi.org/10.1016/j.ijfatigue.2016.10.004>.
- O'Brien, T.K., Rigamonti, M., Zanotti, C., 1989. Tension fatigue analysis and life prediction for composite laminates. *Int. J. Fatigue* 11, 379–393. [https://doi.org/10.1016/0142-1123\(89\)90177-1](https://doi.org/10.1016/0142-1123(89)90177-1).
- Pavan, Acharya, Dayananda, P., Vijaya, K.M., Hegde, S., Narampady Hosagade, P., 2018. Influence of seawater absorption on vibrational and tensile characteristics of quasi-isotropic glass/epoxy composites. *J. Mater. Res. Technol.* 1–7. <https://doi.org/10.1016/j.jmrt.2018.10.008>.
- Rafee, R., 2017. Stochastic fatigue analysis of glass fiber reinforced polymer pipes. *Compos. Struct.* 167, 96–102. <https://doi.org/10.1016/j.compstruct.2017.01.068>.
- Ramesh, Talreja, 2016. In: *Modeling Damage, Fatigue and Failure of Composite Materials*. Woodhead Publications. <https://doi.org/10.1016/B978-1-78242-286-0.00012-1>.
- Reifsnider, K.L., 1991. *Fatigue of Composite Materials*. Elsevier Science Publishing Company Inc..
- Sun, C.T., Zhou, S.G., 1988. Failure of quasi-isotropic composite laminates with free edges. *J. Reinf. Plast. Compos.* 7, 515–557. <https://doi.org/10.1177/073168448800700602>.
- Toubal, L., Karama, M., Lorrain, B., 2006. Damage evolution and infrared thermography in woven composite laminates under fatigue loading. *Int. J. Fatigue* 28, 1867–1872. <https://doi.org/10.1016/j.ijfatigue.2006.01.013>.
- Venkatachalam, S., Murthy, H., 2018. Damage characterization and fatigue modeling of CFRP subjected to cyclic loading. *Compos. Struct.* 0–1. <https://doi.org/10.1016/j.compstruct.2018.05.030>.
- Vieira, P.R., Carvalho, E.M.L., Vieira, J.D., Toledo Filho, R.D., 2018. Experimental fatigue behavior of pultruded glass fibre reinforced polymer composite materials. *Compos. Part B Eng.* 146, 69–75. <https://doi.org/10.1016/j.compositesb.2018.03.040>.
- Wu, F., Yao, W.X., 2010. A fatigue damage model of composite materials. *Int. J. Fatigue* 32, 134–138. <https://doi.org/10.1016/j.ijfatigue.2009.02.027>.
- Zhao, X., Wang, X., Wu, Z., Zhu, Z., 2016. Fatigue behavior and failure mechanism of basalt FRP composites under long-term cyclic loads. *Int. J. Fatigue* 88, 58–67. <https://doi.org/10.1016/j.ijfatigue.2016.03.004>.
- Ziemian, C.W., Ziemian, R.D., Haile, K.V., 2016. Characterization of stiffness degradation caused by fatigue damage of additive manufactured parts. *Mater. Des.* 109, 209–218. <https://doi.org/10.1016/j.matdes.2016.07.080>.
- Zong, J., Yao, W., 2017. Fatigue life prediction of composite structures based on online stiffness monitoring. *J. Reinf. Plast. Compos.* 36, 1038–1057. <https://doi.org/10.1177/0731684417701198>.